Polymer 50 (2009) 2445–2450

Contents lists available at ScienceDirect

Polymer

journal homepage: www.elsevier.com/locate/polymer

Determination of electron inelastic mean free paths for poly[methyl(phenyl)silylene] films

J. Zemek [a,*], J. Houdkova [a], P. Jiricek [a], A. Jablonski [b], V. Jurka [a], J. Kub [a]

[a] *Institute of Physics Academy of Sciences of the Czech Republic, Cukrovarnicka 10, 162 53 Prague 6, Czech Republic*
[b] *Institute of Physical Chemistry, Polish Academy of Sciences, ul. Kasprzaka 44/52, 01-224 Warszawa, Poland*

ARTICLE INFO

Article history:
Received 28 January 2009
Received in revised form
10 March 2009
Accepted 19 March 2009
Available online 27 March 2009

Keywords:
Polymer physics
Poly[methyl(phenyl)silylene]
Inelastic mean free path

ABSTRACT

The inelastic mean free paths (IMFPs) of electrons at a poly[methyl(phenyl)silylene] thin film surface were determined using elastic peak electron spectroscopy (EPES) and Monte Carlo calculations for a wide electron energy range, 200–1600 eV. We considered the surface composition determined from X-ray induced photoelectron spectra (XPS), the hydrogen concentration evaluated by EPES, and a correction for surface excitations. The results compare well to those calculated from the predictive TPP-2M and G1, formulae. Calculations carried out with the quantitative structure–property relationship of Cumpson and the formula of Ashley and Williams provide larger IMFP values, and can be useful only for a rough estimation.

1. Introduction

The inelastic mean free path (IMFP) of electrons passing a near-surface region of a solid is a basic parameter for quantification of electron spectroscopes, AES and XPS [1]. The IMFP determines the sampling depth of these techniques [2,3], and plays a key role in determining the surface composition, and in calculations associated with non-destructive depth profiling [4]. The IMFP can be measured [5] or calculated with the use of various models [6–9].

In the early days of electron spectroscopy, the IMFP was obtained, incorrectly, from measurements of the attenuation of signal electrons originating from a substrate and an overlayer of predetermined thickness. As we know now, the parameter derived in this way is influenced by elastic scattering of electrons, what is now termed the attenuation length [10]. In addition, it was shown later that it is difficult to prepare homogeneous overlayers of comparable thickness to the IMFP. Consequently, overlayer–substrate experiments are not recommended for determining IMFPs [5].

IMFP values, in agreement with the ASTM definition [11] can be determined from measurements and Monte Carlo (MC) calculations of the probability of elastic electron backscattering from a given solid. Elastic peak electron spectroscopy (EPES) is a well-established method for determining IMFP values. Experimentally, a sample is irradiated by well-defined electron beam at a given electron energy. Electrons pass the solid surface, travel given trajectory lengths in the solid, leave the surface and enter the electron energy analyzer. Thus, the elastic-backscattering intensity is recorded. To avoid experimental problems in determining the absolute probability of electron elastic-backscattering, relative measurements of a given sample and a standard have been successfully used [5]. Therefore, in a typical electron spectrometer, the studied sample and a reference sample for which the IMFPs are known at energies of interest are inserted. Experiment provides the ratio of elastic peak intensities for both materials at a given energy and exactly the same experimental geometry. Up to now, the procedure has been applied to a number of elemental solids and inorganic compounds (see Ref. [5] for review).

The published material on IMFPs for organic compounds is rather limited [12–16]. In particular, the IMFP energy dependence has been determined for polyacetylene [12], polyaniline [13,15,16], polythiophene [14,16], and polyethylene [16]. No IMFP data are available for the poly[methyl(phenyl)silylene] (PMPSi) studied in this work. The PMPSi belongs to the family of silicon-based polymers, polysilanes. Polysilanes are of increasing interest owing to their applications, e.g. in electroluminescent devices, sensors, photoconductors, non-linear optical materials, and electron-resist materials suitable for silicon nanotechnologies. Their main advantage is the processibility and modification of their properties by various side groups. Compatibility of polysilanes with both silicon-based

---

* Corresponding author.
E-mail address: zemek@fzu.cz (J. Zemek).

0032-3861/$ – see front matter © 2009 Elsevier Ltd. All rights reserved.
doi:10.1016/j.polymer.2009.03.031

technologies and organic material deposition methods suggests their potential in nanolithography [17–20].

PMPSi is a quasi-one-dimensional material with delocalised σ electrons along the polymer backbone. Its unique electronic properties are attributed to the effect of quantum confinement of these electrons on polymer segments. Besides the applications, electron beam-induced phenomena, important in electron microscopy, electron spectroscopy, and electron lithography, are far from satisfactorily understood, particularly the degradation mechanism [21]. Detailed knowledge of electron transport and electron scattering in PMPSi helps us to gain insight into conditions for the formation of weak bonds, bond scission, and hydrogen evolution due to electron beam interaction. Therefore, knowledge of the IMFP as the main transport parameter for electrons passing near the PMPSi surface is highly desirable.

In the present work, we measured and calculated elastic-backscattering probabilities for electrons incident on the surfaces of PMPSi thin films in order to obtain IMFP values for a wide range of electron energies, from 200 eV to 1600 eV. The resulting electron energy dependence of the IMFP was compared with results calculated using available models.

2. Experimental section

2.1. Materials

Poly[methyl(phenyl)silylene] films (PMPSi, Fig. 1) were prepared by Wurtz coupling polymerization, as described by Zhang and West [22]. The low-molecular weight fractions were extracted with boiling diethyl ether. Thin films were prepared from a toluene solution by casting on silicon and Au-covered silicon substrates under a protective He atmosphere in a small preparation chamber attached to a photoelectron spectrometer. To prevent surface charging during spectra acquisition, the thickness of the films was tailored to be about 20 nm. A sputter-cleaned Cu layer deposited on an Si(111) substrate by vacuum evaporation with a thickness of about 400 nm was used as a standard for the EPES measurements.

The density of the PMPSI film was estimated by two independent methods, as follows:

(a) by analytical weighing of the film deposited on a silicon wafer and by estimating the volume of the film. The film thickness was measured by a stylus method and by cross-sectional electron microscopy.
(b) by grazing-angle X-ray reflectivity (XRR). From the measurement of the critical angle for total external reflection, the total electron density can be measured, from which the mass density can be derived directly [23,24]. The XRR curves were measured on D8 discovery diffractometer (Bruker AXS) with a parallel beam (parabolic Goebel mirror) and knife-edge towards the sample surface. The source was a copper target X-ray tube.

The PMPSi film density used in the calculations accompanying the EPES procedure was taken as the average value from the above-mentioned methods, which was estimated as $1.2 \pm 0.1\ \mathrm{g\,cm^{-3}}$. This value is close to that reported, $1.078\ \mathrm{g\,cm^{-3}}$ [25].

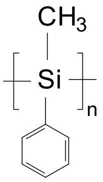

Fig. 1. The chemical formula for PMPSi.

2.2. Measurement

The EPES and XPS spectra were recorded with an ADES 400 angle-resolved photoelectron spectrometer (VG Scientific, UK) equipped with an electron gun (Varian, model 981-2455), Mg Kα and Al Kα excitation sources, and a rotatable hemispherical electron energy analyzer. During the EPES measurements, the electron beam incidence angle was normal to the sample surface. The emission angle was set to 35° from the surface normal. Electron elastic peak spectra were excited by a defocused electron beam with energies of 200, 250, 300, 350, 400, 500, 750, 1000, 1200, 1400, and 1600 eV, a beam current of 4×10^{-9} to 1×10^{-7} A, a spot diameter at the sample surface of 3 mm, and a data-acquisition time was typically 30 s per sample and a given electron energy. A higher value of beam current up to 1×10^{-7} A was used at high electron energies where the EPES intensities are small. In addition, a primary beam energy of 1500 eV, a beam current of 1×10^{-6} A, and a data-acquisition time of 180 s were used to estimate the percentage of hydrogen in the samples [26]. Elastically backscattered electrons were collected from the PMPSi surfaces and from a copper surface considered as the recommended reference [5] at a pass energy of 20 eV within a small conical analyzer acceptance angle of ±4°. The typical width of the elastic peak was about 0.5 eV (FWHM). The elastic peak intensities were isolated from the inelastic background using the Shirley background subtraction technique [27]. The surface composition of the PMPSi surfaces and the surface cleanness of the Cu standard were checked by XPS.

3. Calculations

3.1. Model calculations

A convenient tool for calculating the IMFP for any solid is the predictive formula known under the acronym TPP-2M [7]. For any material, the IMFP can be calculated from the following set of equations

$$\lambda = \frac{E}{E_p^2\left[\beta \ln(\gamma E) - (C/E) + \left(D/E^2\right)\right]} \tag{1}$$

where E is the electron energy (in eV). The remaining parameters are defined by

$$E_p = 28.8(N_v \rho / M)^{1/2} \tag{2}$$

$$\beta = -0.10 + 0.944/\left(E_p^2 + E_g^2\right)^{1/2} + 0.069\,\rho^{0.1} \tag{3}$$

$$\gamma = 0.191\,\rho^{-0.50} \tag{4}$$

$$C = 1.97 - 0.91\,U \tag{5}$$

$$D = 53.4 - 20.8\,U \tag{6}$$

$$U = N_v \rho / M = E_p^2 / 829.4 \tag{7}$$

where N_v is the number of valence electrons per atom or molecule, ρ is the material density (in g/cm^3), and M is the atomic or molecular weight, and E_g is the band-gap energy (in eV) for non-conductors. The IMFP values were calculated using the NIST Database SRD 82 [10] with the following input parameters: $N_v = 40$, $E_g = 5.0$ eV [20], and the volume density of PMPSi, ρ determined experimentally.

A relevant method for predicting IMFP values for polymers and other organic materials was published by Cumpson [8]. This approach involves a quantitative structure–property relationship, which allows the IMFP to be estimated for any organic material from its structural formula alone. It is based on the Kier–Hall molecular indices [28,29]. Cumpson [8] developed a simple expression for the IMFP

$$\lambda(1\ \mathrm{keV}) = \left[a\left({}^{0}\chi^{(\nu)}\right) + bN_{\mathrm{rings}}\right]/N_{\text{non-H}} + c \tag{8}$$

where ${}^{0}\chi^{(\nu)}$ is the zero-order or atomic connectivity indices of Kier and Hall, evaluated by Bicerano's method [28]. In the case of a polymer, $N_{\text{non-H}}$ is the number of atoms in the molecule or polymer repeat unit, excluding hydrogen atoms, N_{rings} is the number of six-member aromatic rings in the molecule or polymer repeat unit, and a, b, c are fitting parameters. A least-squares fit of Eq. (8) to the IMFP values for polymers tabulated by Tanuma et al. [30] from optical data gives

$$\lambda(1\ \mathrm{keV}) = \left[3.117\left({}^{0}\chi^{(\nu)}\right) + 0.4207N_{\mathrm{rings}}\right]/N_{\text{non-H}} + 1.104\ (\mathrm{nm}) \tag{9}$$

Eq. (9) can easily be extended to other energies using the power-law dependence of the IMFP.

$$\lambda = aE^{p} \tag{10}$$

where a and p are the constants. The exponent p varies in a relatively wide range. Tanuma et al. [7] found $p = 0.79$ for their group of 14 organic compounds while Jablonski [31] proposed $p = 0.7665$ as the average energy dependence of IMFP for organic compounds. The latter value was used in the present calculation. Note that the power-law dependence has no physical justification [31]. However, it describes the energy dependence of IMFP reasonably well over a relatively narrow energy range. Subsequently,

$$\lambda(E) = \left\{\left[3.117\left({}^{0}\chi^{(\nu)}\right) + 0.4207N_{\mathrm{rings}}\right]/N_{\text{non-H}} + 1.104\right\}E^{p}\ (\mathrm{nm,\ keV}) \tag{11}$$

Another useful method for predicting IMFP values for inorganic and organic materials was formulated by Gries [9] based on an orbital model. This method essentially states that the IMFP of an electron traversing matter is inversely proportional to the atomic density. The energy dependence of the IMFP and the best values for two fitting parameters were obtained from a large set of IMFPs derived by Tanuma et al. [30] from published optical data. The so-called G1 equation expresses the IMFP as

$$\lambda = k_1\left(V_{\mathrm{a}}/Z^{*}\right)E/(\log_{10}E - k_2) \tag{12}$$

where V_{a} is the atomic volume in $\mathrm{cm^3\,mol^{-1}}$, E is the energy of an analytical electron in eV, $k_1$and k_2 are numerical fitting parameters derived from the optical IMFPs of TPP, and Z^{*} is a real number which can be regarded as the nominal "effective" number of interaction-prone electrons per atom. For electron energies between 200 and 2000 eV and for organic compounds, $k_1 = 0.0018$ and $k_2 = 1.00$. The λ values from Eq. (12) were calculated using the NIST Database SRD 82 [10] with the volume density of PMPSi, ρ, as the input parameter.

Ashley and Williams [6] derived a simple expression for the IMFP of electrons in solid organic insulators. The IMFP is considered, as a good approximation, to be inversely proportional to the valence electron density for a given electron energy.

$$\lambda N = E/[152\ \ln E - 235 - 920/E] \tag{13}$$

$$N = 0.0891\ \rho N_{\mathrm{v}}/M$$

where ρ is the density of the material in $\mathrm{g\,c\,m^{-3}}$, M is the molecular weight of the molecule or monomeric unit in grams per mole, and N_{v} is the number of valence electrons per molecule or monomeric unit.

3.2. Monte Carlo calculations

Elastic peak electron spectroscopy is mainly used for determining the IMFP of various materials, including polymers. The relevant experiments provide ratios of the elastic-backscattering probabilities (which are equal to the ratio of the elastic peak intensities) for the studied sample and for the standard material. The same ratio is calculated from a realistic model of electron transport in a solid that accounts for multiple elastic electron scattering. Calculations are performed for various IMFPs assumed for the sample. The IMFP for this sample is obtained by comparing the measured ratio with the calculated ratios for a given energy. The theoretical models and the relevant algorithms have been extensively reviewed in the literature [5,32]. In the present work, the MC calculations were performed using the EPESWIN software packet [33], the recommended IMFP values for the Cu standard [5,34], and elastic-scattering cross-sections for the target atoms from the NIST electron elastic-scattering cross-section database [35]. The remaining input parameters are: the experimental geometry used (incidence and emission angle, analyzer solid angle), the sample surface composition evaluated from XPS/EPES spectra, and the measured sample volume density.

4. Results and discussion

Atomic concentrations were determined from the electron inelastic-background-subtracted photoelectron peak areas of the C 1s, O 1s, and Si 2p lines corrected for photoelectron cross-sections [36], inelastic mean free paths [7], and the experimentally determined transmission function of the hemispherical electron energy analyzer [37]. The experimental uncertainties accompanying XPS quantitative analysis were estimated to be $\leq$7%. This value covers overall uncertainties of the method, which are mostly introduced by the background subtraction and the correction procedure used for calculating concentrations from intensities of the spectral lines.

Hydrogen cannot be analyzed and quantified by XPS. For this reason, the concentration of hydrogen was evaluated from the EPES spectrum recorded at a primary electron beam energy of 1500 eV, and at an emission angle of 35°, i.e. for a scattering angle of 145°. The spectrum is shown in Fig. 2. The dominant peak is unresolved due to electrons backscattered elastically by carbon, silicon and oxygen atoms. The minor peak, shifted by 2.7 eV with respect to the major peak, originates from electrons elastically scattered on hydrogen atoms. The shift, associated with the recoil of elastically backscattered electrons by light target atoms, is in accord with the value predicted by theory [26]. Consequently, the electron-atom elastic collision is not, in fact, strictly elastic. The atomic percentage of hydrogen was calculated from the ratio of the two above-mentioned elastic peak areas, the major and minor peaks, corrected for the appropriate elastic-scattering cross-sections [35] and provided that the sample composition is homogeneous over the analyzed volume [26]. The results are summarized in Table 1 and are compared with the expected values derived from the structural formula (Fig. 1). The results differ in hydrogen percentage and in the carbon-to-silicon ratio, due likely to electron beam-induced bond scission and hydrogen loss from the film surface during EPES spectrum acquisition [38]. The reduced hydrogen content in the analyzed volume was expected and verified experimentally. The hydrogen depletion has, however, little effect on the resulting IMFP values, because (i) the electron dose used for EPES measurements was considerably lower than for the hydrogen estimation and (ii)

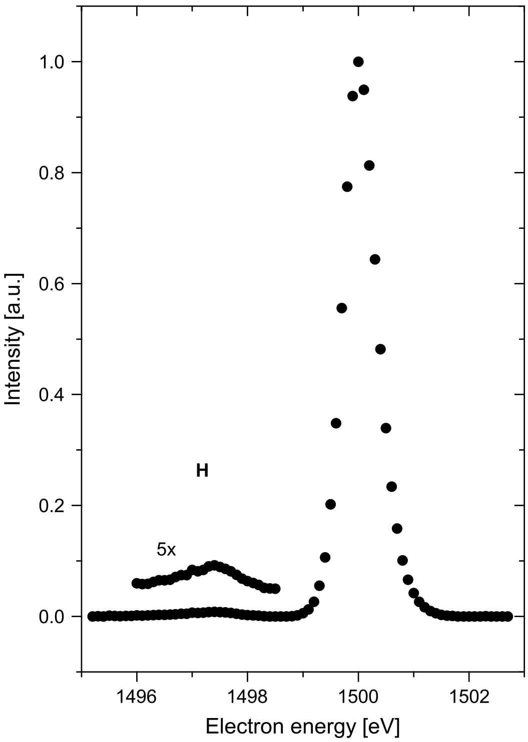

Fig. 2. Typical spectra of elastically backscattered electrons recorded from the PMPSi surface at an electron primary beam energy of 1500 eV and a scattering angle of 145°. A tiny peak at 1497.3 eV originates from electrons quasi-elastically scattered on hydrogen atoms.

the electron elastic-scattering cross-section for hydrogen atoms is much smaller than the values for carbon, silicon and oxygen at the same electron energy and scattering angle [35]. From the former it follows that the hydrogen depletion from a surface region of the PMPSi would be weaker than for the conditions used for the hydrogen estimation. From the latter one can deduce that the expected reduced electron intensity from hydrogen has a little influence on the overall elastic peak intensity.

The IMFP values are evaluated from a comparison of measured and MC-calculated electron elastic-backscattering probabilities. The electron energy dependence of the peak-area ratios of the elastic peaks for PMPSi relative to Cu for both uncorrected and surface-excitation-corrected experimental data is shown in Fig. 3. The plots decrease monotonously with electron energy, similar to the corresponding ratio of the differential cross-sections for electron elastic scattering (bottom plot) [35].

It has been known [39], however, that surface excitations reduce the intensity of signal electrons by a factor exp($-P_s$), where P_s is the surface-excitation parameter [40]. In EPES, electrons entering the analyzer, after traveling a given trajectory length in the solid, pass the surface region twice, which increases the probability of surface energy loss, as compared with a trajectory of the same length traveled in the bulk of the solids. The probability of no energy loss on a trajectory is decreased by the following factor [41]

$$f_s = \exp\left[-P_s^{\text{in}}\left(\alpha^{\text{in}}, E\right)\right] \ \exp\left[-P_s^{\text{out}}\left(\alpha^{\text{out}}, E\right)\right] \qquad (14)$$

where the superscripts "in" and "out" indicate the direction of an electron with respect to the surface and α is the emission angle.

Table 1
Comparison of the nominal and measured surface compositions in at. % of the analyzed PMPSi film.

Element composition ⇓	H	C	Si	O	C/Si
Nominal	50	43.75	6.25	–	7
XPS	40.0	51.0	8.5	0.5	6

Werner et al. [42,43] derived a simple empirical expression from Oswald's calculations [44] describing P_s for various materials

$$P_s(\alpha, E) = \frac{1}{0.173\ aE^{1/2}\cos\alpha + 1} \qquad (15)$$

where a is a material-dependent parameter. To introduce surface energy losses into the algorithm for calculating the IMFP, we need to divide the measured ratio of intensities by the surface-excitation correction (Fig. 3)

$$K = \frac{f_s^{\text{PMPSi}}}{f_s^{\text{Cu}}} \qquad (16)$$

In the present analysis, we estimate the value of the material parameter for PMPSi from the approximate expression proposed by Werner et al. [42,43] and modified by Pauly and Tougaard for non-conductors [45]

$$a = 0.039\ E_p + 0.4 + 0.22\ E_g = 2.21 \qquad (17)$$

where E_p is the bulk plasmon energy defined by Eq. (2) and E_g is the energy gap. The corresponding value for Cu, $a = 1.23$, was taken from Ref. [46]. The energy dependence of the measured peak-area ratios, uncorrected and corrected for surface-excitation effects, is shown in Fig. 3. The corrected ratios are slightly shifted to lower values for all electron energies considered. Therefore, the resulting IMFP values evaluated from the corrected ratios would be shifted to lower values with respect to the uncorrected data.

Resulting values of IMFPs derived from the measured corrected and uncorrected EPES data and MC calculations are compared in Fig. 4 with those calculated using the approaches of TPP-2M [7],

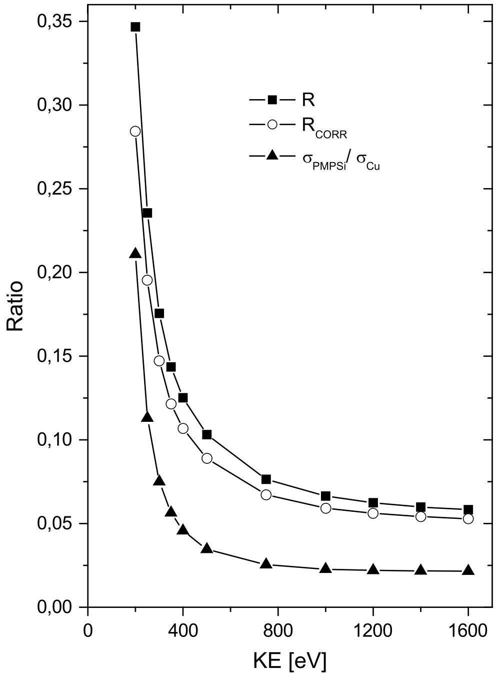

Fig. 3. Energy dependence of elastic peak intensity ratios for PMPSi relative to Cu, uncorrected and corrected for electron inelastic surface losses. The bottom plot represents the energy dependence of the differential elastic cross-section ratios for both materials.

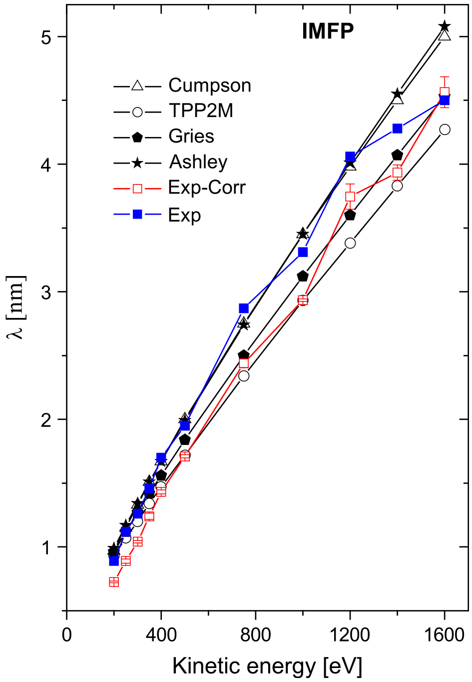

Fig. 4. Energy dependence of the inelastic mean free paths derived from the EPES experiments and Monte Carlo calculations of electron elastic-backscattering probabilities using the uncorrected (filled squares, blue on-line) and surface energy-loss-corrected (empty squares, red on-line) intensity ratios from Fig. 3. IMFPs are also shown from the TPP-2M formula [7], the quantitative structure–property relationship [8], the G1 predictive formula of Gries [9], and the formula of Ashley and Williams [6]. The error bars the empty squares (red on-line) indicate the uncertainties from the MC calculations (statistical errors evaluated as a standard deviation from 5 times calculated IMFPs at a given electron energy).

Cumpson [8], Gries [9], and Ashley and Williams [6]. The IMFPs increase with electron energy, as expected. Whereas the uncorrected data points are close to the Cumpson calculations and the Ashley and Williams formula, the surface-excitation-corrected data are closer to the TPP-2M and Gries, formulae. Note, the corrected data and the TPP-2M/Gries data deviate more widely at low electron energy. This indicates a systematic error in the correcting procedure accounting for the surface-excitation effects. The numerical IMFP data, corrected for surface-excitation effects, are also available in Table 2. Here and also in Fig. 4, the data are presented as the mean values with standard deviations from five MC calculations at each electron energy. The standard deviations indicate statistical errors of the MC calculations. Experimental uncertainties associated with measurements of elastic peak areas of the PMPSi and the Cu and their background subtraction were found to be marginal, typically below 1%, because we used the high-energy resolution electron energy analyzer with typical width (FWHM) of elastic peaks ∼0.5 eV and a low background level.

Table 2
Numerical results of the IMFP for electrons traversing PMPSi films. The data are presented as the mean values with standard deviations from five MC calculations at each electron energy and are corrected for surface-excitation losses.

Electron energy [eV]	IMFP [nm]
200	0.73 ± 0.01
250	0.89 ± 0.02
300	1.04 ± 0.01
350	1.24 ± 0.02
400	1.43 ± 0.01
500	1.71 ± 0.02
750	2.44 ± 0.03
1000	2.93 ± 0.01
1200	3.75 ± 0.10
1400	3.93 ± 0.06
1600	4.56 ± 0.12

5. Conclusions

The energy dependence of inelastic mean free paths was determined by measurements and MC calculations of electron elastic-backscattering probabilities. The measured data were evaluated considering the surface composition, including the hydrogen concentration and corrected for surface inelastic energy losses. The results compare well to those calculated from the predictive TPP-2M [Eq. (1)] and G1 [Eq. (12)], formulae. Calculations carried out with the quantitative structure–property relationship of Cumpson and the formula of Ashley and Williams provide larger IMFP values, and can be useful only for a rough estimation.

Acknowledgement

This work was supported by the Grant Agency of the Academy of Sciences of the Czech Republic, Project No. IAA100100622, Czech Science Foundation Project No. 202/09/0428, and Institutional Research Plan No. AV0Z10100521. One of the authors (A.J.) wishes to acknowledge support for part of the work from grant N N204 0769 33.

References

[1] Fadley CS, Baird RJ, Novakov T, Bergstrom SAL. J Electron Spectrosc Rel Phenom 1974;4:93–137.
[2] Zemek J, Hucek S, Jablonski A, Tilinin IS. J Electron Spectrosc Relat Phenom 1995;76:443–7.
[3] Jablonski A, Powell CJ. J Vac Sci Technol A 2003;21:274–83.
[4] Cumpson PJ. J Electron Spectrosc Relat Phenom 1995;73:25–52.
[5] Powell CJ, Jablonski A. J Phys Chem Ref Data 1999;28:19–62.
[6] Ashley JC, Williams MW. Radiat Res 1980;81:364–73.
[7] Tanuma S, Powell CJ, Penn DR. Surf Interface Anal 1994;21:165–76.
[8] Cumpson PJ. Surf Interface Anal 2001;31:23–34.
[9] Gries WH. Surf Interface Anal 1996;24:38–50.
[10] Powell CJ, Jablonski A. NIST electron effective-attenuation-length database (SRD 82). v. 1.1. Gaithersburg, MD: NIST, <http://www.nist.gov/srd/nist82.htm>; 2003.
[11] Standard E 673-03. Annual book of ASTM standards 2008. v. 3.06. West Conshohocken, PA: ASTM International; 2008. p. 675.
[12] Lesiak B, Kosinski A, Krawczyk M, Zommer L, Jablonski A, Zemek J, et al. Appl Surf Sci 1999;144–145:168–72.
[13] Lesiak B, Jablonski A, Zemek J, Trchova M, Stejskal J. Langmuir 2000;16:1415–23.
[14] Lesiak B, Kosinski A, Jablonski A, Kover L, Toth J, Varga D, et al. Appl Surf Sci 2001;174:70–85.
[15] Lesiak B, Jablonski A, Kosinski A, Kover L, Toth J, Varga D, et al. Surf Sci 2002;507:900–5.
[16] Gergely G, Menyhard M, Orosz GT, Lesiak B, Kosinski A, Jablonski A, et al. Appl Surf Sci 2006;252:4982–9.
[17] Maeda K, Seki S, Tagawa S, Shibate H. Rad Phys Chem 2001;60:461–6.
[18] Hayase S. Prog Polym Sci 2003;28:359–81.
[19] Okazaki A, Akita S, Nishijima H, Nakayama Y. Jpn J Appl Phys 2000;39:3744–6.
[20] Matsumoto N, Suzuki H, Miyazaki H. In: Jones RG, Ando W, Chojnowski J, editors. Silicon-containing polymers. The science and technology of their synthesis and application. Kluwer Academic Publishers; 2000.
[21] Kuritka I, Horvath P, Schauer F, Zemek J. Polym Degrad Stabil 2006;91:2901–10.
[22] Zhang XH, West R. J Polymer Sci Polym Chem Ed 1984;22:159–70.
[23] Ferrari AC, Libassi A, Tanner BK, Stolojan V, Yuan J, Brown LM, et al. Phys Rev B 2000;62:11089–103.
[24] Huang TC, Gilles R, Will G. Thin Solid Films 1993;230:99–101.
[25] Herden V, Klaumunzer S, Schnabel W. Nucl Instrum Meth B 1998;146:491–5.
[26] Lesiak B, Zemek J, Houdkova J. Polymer 2008;49:4127–32.
[27] Shirley DA. Phys Rev B 1972;5:4709–14.
[28] Bicerano J. Prediction of polymer properties. 2nd ed. New York: Marcel Dekker; 1996.
[29] Kier LB, Hall LH. Molecular structure description. San Diego, CA: Academic Press; 1999.
[30] Tanuma S, Powell CJ, Penn DR. Surf Interface Anal 1991;17:927–39.
[31] Jablonski A. Surf Interface Anal 1993;20:317–21.
[32] Dubus A, Jablonski A, Tougaard S. Progr Surf Sci 2000;63:135–75.
[33] Jablonski A. Surf Interface Anal 2005;37:1035–44.
[34] Powell CJ, Jablonski A. NIST electron inelastic-mean-free-path database (SRD 71). v. 1.1. Gaithersburg, MD: NIST, <http://www.nist.gov/srd/nist71.htm>; 2000.

[35] Jablonski A, Salvat F, Powell CJ. NIST electron elastic-scattering cross-section database (SRD 64). v. 3.1. Gaithersburg, MD: NIST, <http://www.nist.gov/srd/nist64.htm>; 2003.
[36] Scofield JH. J Electron Spectrosc Relat Phenom 1976;8:129–37.
[37] Jiricek P. Czech J Phys 1994;44:261–7.
[38] Filippi M, Calliari L. Surf Interface Anal 2008;40:1469–74.
[39] Yubero F, Tougaard S. Phys Rev B 1992;46:2486–97.
[40] Chen YF. Surf Sci 1997;380:199–209.
[41] Tanuma S, Ichimura S, Goto K. J Surf Anal 1999;5:48–52.
[42] Werner WSM, Smekal W, Tomastik C, Stori H. Surf Sci 2001;486:L461–6.
[43] Werner WSM. Surf Interface Anal 2001;31:141–76.
[44] Oswald R. Ph.D. Thesis. Eberhard-Karls-Universitat, Tubingen; 1992.
[45] Pauly N, Tougaard S. Surf Interface Anal 2008;40:731–3.
[46] Pauly N, Tougaard S. Surf Sci 2007;601:5611–5.